

Usefulness of effective field theory for boosted Higgs production

S. Dawson

Department of Physics, Brookhaven National Laboratory, Upton, N.Y., 11973, U.S.A.

I. M. Lewis

SLAC National Accelerator Laboratory, Menlo Park, CA, 94025, U.S.A.

Mao Zeng

*C.N. Yang Institute for Theoretical Physics,
Stony Brook University, Stony Brook, N.Y., 11794, U.S.A.*

Abstract

The Higgs + jet channel at the LHC is sensitive to the effects of new physics both in the total rate and in the transverse momentum distribution at high p_T . We examine the production process using an effective field theory (EFT) language and discuss the possibility of determining the nature of the underlying high scale physics from boosted Higgs production. The effects of heavy color triplet scalars and top partner fermions with TeV scale masses are considered as examples and Higgs-gluon couplings of dimension-5 and dimension-7 are included in the EFT. As a by-product of our study, we examine the region of validity of the EFT. Dimension-7 contributions in realistic new physics models give effects in the high p_T tail of the Higgs signal which are so tiny that they are likely to be unobservable.

I. INTRODUCTION

The recently discovered Higgs boson has all the generic characteristics of a Standard Model (SM) Higgs boson and measurements of the production and decay rates agree to the $\sim 20\%$ level with Standard Model predictions [1–4]. Precision measurements of Higgs couplings are essential for understanding whether there exist small deviations from the Standard Model predictions which could be indications of undiscovered high scale physics. If there are no weak scale particles beyond those of the SM, then effective field theory (EFT) techniques can be used to probe the Beyond the Standard Model (BSM) physics [5–7]. The EFT is the most general description of low energy processes and new physics manifests itself as small deviations from the SM predictions. In the electroweak sector, this approach has been extensively studied [8–12]. The effects of BSM operators affecting Higgs production in the strong sector have been less studied [13–15].

The largest contribution to Standard Model Higgs boson production at the LHC comes from gluon fusion through a top quark loop and we examine new physics effects in this channel, along with the related Higgs + jet channel. We consider an effective Lagrangian containing the SM fermions and gauge bosons, along with a single Higgs boson, h . At dimension-4, the fermion- Higgs couplings can be altered from the SM couplings by a simple rescaling,

$$-\mathcal{L}_f = \kappa_f \left(\frac{m_f}{v} \right) \bar{f} f h + H.c. , \quad (1)$$

where $\kappa_f = 1$ in the SM. In models with new physics, the gluon fusion rate can also be altered by new heavy particles interacting with the Higgs boson at one-loop, which contribute to an effective dimension-5 operator [16–18]

$$\mathcal{L}_5 = C_1 G^{A,\mu\nu} G_{\mu\nu}^A h , \quad (2)$$

where $C_1 = \alpha_s/(12\pi v)$ for an infinitely heavy fermion with $\kappa_f = 1$. For convenience, we define κ_g to be the ratio of C_1 to this reference value,

$$\kappa_g \equiv C_1 / \left(\frac{\alpha_s}{12\pi v} \right) . \quad (3)$$

We compute the top quark contribution to scattering processes exactly using Eq. 1, (*i.e.*, not in the infinite top quark mass limit), and consider C_1 to be only the contribution from new physics. The measurement of gluon fusion by itself can determine a combination of κ_g

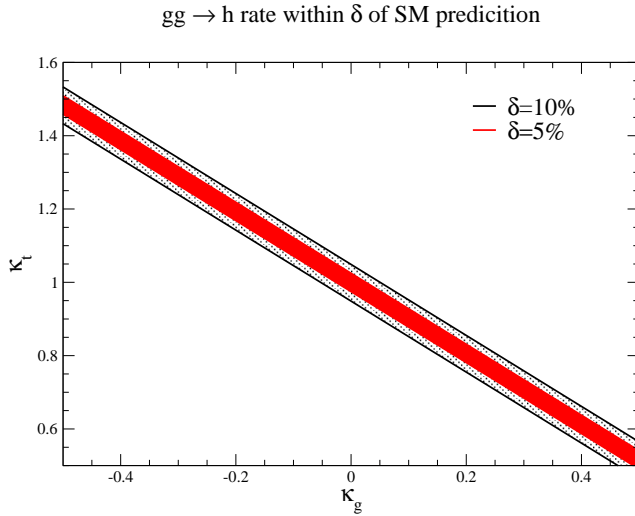


FIG. 1: Allowed values of the EFT coefficients when the total gluon fusion rate, $gg \rightarrow h$, is within $\pm 10\%$ ($\pm 5\%$) of the SM prediction, ($\kappa_g \equiv 12\pi v C_1/\alpha_s$).

and the top quark Yukawa coupling, κ_t , but cannot distinguish between the two for $m_t \gg m_h$ [19–22]. Including the dimension-5 operator of Eq. (2), the cross section is generically,

$$\mu_{ggh} \equiv \frac{\sigma(gg \rightarrow h)}{\sigma(gg \rightarrow h)_{SM}} \sim |\kappa_t + \kappa_g|^2 + \mathcal{O}\left(\frac{m_h^2}{m_t^2}\right). \quad (4)$$

The requirement that $|\mu_{ggh} - 1| < 10\%$ (or 5%) is shown in Fig. 1, where top quark mass effects are included exactly. The SM corresponds to the point $\kappa_g = 0, \kappa_t = 1$. The contribution from b -quarks is small and has been neglected.

The boosted production of the Higgs boson through the process $pp \rightarrow h + \text{jet}$ is sensitive to the Higgs-gluon effective coupling [20–25] and offers the possibility of disentangling new physics effects and hence breaking the degeneracy between κ_t and κ_g . An effective

Lagrangian approach is useful for studying this high p_T BSM physics and the Higgs-parton interactions can be described as a sum of higher dimension operators,

$$\mathcal{L}_{EFT} \sim \mathcal{L}_4 + \mathcal{L}_5 + \mathcal{L}_6 + \mathcal{L}_7 + \dots, \quad (5)$$

where \mathcal{L}_n includes all dimension- n operators. At dimension-5 and assuming CP conservation, there is only the single operator of Eq. (2) modifying the Higgs-gluon interactions. The dimension-5 operator has been broadly used to obtain higher order QCD corrections to Higgs rates [17, 18, 26–32].

Dimension-7 operators affecting Higgs- gluon interactions from QCD interactions have received less attention [14, 33, 34]. Because their contributions are proportional to the strong coupling, g_s , these operators can have numerically significant effects. In a previous work [13], we considered the effects of dimension-7 operators affecting Higgs- gluon interactions and demonstrated the importance of including these operators along with the NLO QCD corrections in order to obtain realistic predictions of boosted Higgs spectra. The largest contribution to Higgs + jet production is from the O_1 operators in the gg initial channel. The NLO QCD corrections to this channel are relatively flat in p_T and lead to an enhancement of roughly a factor of 2 in the rate at the 14 TeV LHC. The contributions from O_3 to Higgs + jet production are suppressed at lowest order QCD (LO) for large p_T , since they vanish in the soft Higgs limit. These contributions receive large NLO corrections, but remain numerically small and are never important. The contributions from the interference of the O_1 and O_5 operators can be important for large $p_T \sim 300 \text{ GeV}$ and receive NLO QCD corrections which are again fairly p_T independent and increase the rate by a factor of ~ 1.2 .

In this paper, we examine the expected size of the coefficients of the Higgs-gluon EFT dimension-5 and dimension-7 operators in several representative UV models with heavy colored scalars and fermions. We are particularly interested in the question of whether the measurement of the boosted Higgs p_T distribution can distinguish the nature of the underlying UV physics, should there be any deviation from the SM. We then demonstrate how the inclusion of the dimension-7 operators affects fit to EFT Higgs parameters from gluon fusion. We work at LO QCD.

In Section II, we review the EFT. The heavy colored scalar and fermion models which we study are introduced in Section III and the matching coefficients of the EFT presented. Phenomenological results at the LHC are given in Section IV and some conclusions about

the usefulness of the EFT in this channel presented in Section V.

II. EFFECTIVE LAGRANGIAN

In this section, we review the effective Lagrangian relevant for Higgs + jet production containing non-SM Higgs-gluon interactions. We consider a CP conserving Lagrangian, with no new Higgs particles,

$$\mathcal{L} = \mathcal{L}_{SM} + (\kappa_t - 1)(-1)\bar{t}t h + \mathcal{L}_5 + \mathcal{L}_7 + \dots, \quad (6)$$

where

$$\mathcal{L}_5 + \mathcal{L}_7 \equiv \hat{C}_1 O_1 + \sum_{i=2,3,4,5} \hat{C}_i O_i, \quad (7)$$

Note that there are no relevant dimension-6 operators of the type we are considering.

At dimension-5, the unique operator is

$$O_1 = G_{\mu\nu}^A G^{\mu\nu,A} h, \quad (8)$$

where $G_{\mu\nu}^A$ is the gluon field strength tensor. The dimension-7 operators needed for the gluon fusion production of Higgs are [33–35],

$$O_2 = D_\sigma G_{\mu\nu}^A D^\sigma G^{A,\mu\nu} h \quad (9)$$

$$O_3 = f_{ABC} G_\nu^{A,\mu} G_\sigma^{B,\nu} G_\mu^{C,\sigma} h \quad (10)$$

$$O_4 = g_s^2 h \sum_{i,j=1}^{n_{lf}} \bar{\psi}_i \gamma_\mu T^A \psi_i \bar{\psi}_j \gamma^\mu T^A \psi_j \quad (11)$$

$$O_5 = g_s h \sum_{i=1}^{n_{lf}} G_{\mu\nu}^A D^\mu \bar{\psi}_i \gamma^\nu T^A \psi_i, \quad (12)$$

where our convention for the covariant derivative is $D^\sigma = \partial^\sigma - i g_s T^A G^{A,\sigma}$, $Tr(T^A T^B) = \frac{1}{2} \delta_{AB}$ and $n_{lf} = 5$ is the number of light fermions. Including light quarks, O_4 and O_5 are needed, which are related by the equations of motion (eom) to gluon-Higgs operators,

$$\begin{aligned} O_4 |_{eom} &\rightarrow D^\sigma G_{\sigma\nu}^A D_\rho G^{A,\rho\nu} h \equiv O'_4 \\ O_5 |_{eom} &\rightarrow G_{\sigma\nu}^A D^\nu D^\rho G_\rho^{A,\sigma} h \equiv O'_5. \end{aligned} \quad (13)$$

Since O_4 involves 4 light fermions, the operator only contributes to Higgs + jet production starting at NLO.

A different dimension- 7 operator is useful,

$$O_6 = -D^\rho D_\rho (G_{\mu\nu}^A G^{\mu\nu,A}) h = -\partial^\rho \partial_\rho (G_{\mu\nu}^A G^{\mu\nu,A}) h = m_h^2 O_1, \quad (14)$$

where the last equal sign is only valid for on-shell Higgs production. Using the Jacobi identities,

$$O_6 = m_h^2 O_1 = -2O_2 + 4g_s O_3 + 4O_5. \quad (15)$$

Therefore, we can choose $O_6 = m_h^2 O_1$, O_3 , O_4 , and O_5 as a complete basis for the dimension-7 Higgs-gluon-light quark operators. We rewrite Eq. (7) as

$$\mathcal{L}_{\text{eff}} = C_1 O_1 + (C_3 O_3 + C_4 O_4 + C_5 O_5). \quad (16)$$

The lowest order amplitudes for Higgs + jet production including all fermion mass dependence (bottom and top) are given in Refs. [36, 37]. A study of Higgs + jet production at LO QCD in the EFT approximation involves only C_1 , C_3 and C_5 [13, 38]. At the lowest order in α_s , O_3 is the only dimension-7 operator which contributes to the $gg \rightarrow gh$ channel, while O_5 is the only dimension-7 operator which contributes to channels with initial state quarks. The lowest order amplitudes in the EFT for Higgs + jet production can be found in Ref. [13], along with the NLO results including the effects of dimension-7 operators. For Higgs + jet production at NLO in BSM models, the EFT description also needs to include the higher-dimensional 3-gluon effective vertex generated at one-loop [13, 39], which could affect dijet and top quark rates [40].

III. UV PHYSICS AND THE EFT

In this section, we discuss several prototype BSM physics models which have heavy particles contributing to Higgs + jet production and we compute the matching coefficients for the EFT in these models. This will allow us to estimate the size of BSM contributions.

A. Heavy Colored Scalars

We consider the addition of either real or complex $SU(3)$ scalars, ϕ_i [41–45]. Our numerical results are all derived for a complex scalar triplet. The scalar portion of the Lagrangian involving a new complex scalar, ϕ_i , and the SM-like Higgs doublet, H , is ,

$$V_{\text{complex}} = V_{SM}(H) + m_i^2 \phi_i^\dagger \phi_i + \frac{C_h}{v} \phi_i^\dagger \phi_i (H^\dagger H) - \lambda_4 (\phi_i^\dagger \phi_i)^2, \quad (17)$$

where V_{SM} is the SM Higgs potential. For a real scalar,

$$V_{\text{real}} = V_{SM} + \frac{m_i^2}{2} (\phi_i)^2 + \frac{C_h}{2v} (\phi_i)^2 (H^\dagger H) - \lambda_4 (\phi_i)^4. \quad (18)$$

In unitary gauge, $H \rightarrow (0, (h + v)/\sqrt{2})$.

B. Top Partner Model

Many BSM contain a charge - $\frac{2}{3}$ partner of the top quark. We consider a general case with a vector-like $SU(2)_L$ singlet fermion which is allowed to mix with the Standard Model like top quark [46–50]. The mass eigenstates are defined to be t and T with masses m_t and M_T and are derived from the gauge eigenstates using bi-unitary transformations involving two mixing angles θ_L and θ_R . Without loss of generality, θ_R can be removed by a redefinition of the top partner gauge eigenstate and the Higgs couplings are then modified from those of the SM [51]:

$$L_h^{top\ partner} = - \left\{ \cos^2 \theta_L \frac{m_t}{v} \bar{t}_L t_R h + \sin^2 \theta_L \frac{M_T}{v} \bar{T}_L T_R h + \frac{M_T}{2v} \sin(2\theta_L) \bar{t}_L T_R h + \frac{m_t}{2v} \sin(2\theta_L) \bar{T}_L t_R h + H.c. \right\}. \quad (19)$$

Precision electroweak fits to the oblique parameters, as well as M_W , place stringent restrictions on the product $\sin^2 \theta_L M_T^2$ and for $M_T \sim 1$ TeV, $\sin \theta_L < .17$ [48, 50]. Higgs production has been investigated at NNLO for top partner models in Ref. [50] and the rate determined to be within a few % of the SM rate for allowed values of θ_L . Large effects in this channel require values of $\sin \theta_L$ that are excluded by precision measurements. ATLAS [52] and CMS [53] have searched for top singlet partners and excluded M_T below 655 GeV and 687 GeV, respectively. Similar limits on top partner masses and mixing can be obtained for different choices of top partner $SU(2)_L$ properties [48].

C. Predictions for Coefficients

The exact results for the contributions from high scale fermion [36, 37] and scalar loops [41, 42] to the rates for $q\bar{q} \rightarrow gh$ and $gg \rightarrow gh$ are well known. Matching to the EFT expressions, the coefficient functions can be extracted. The EFT amplitude for $q\bar{q} \rightarrow gh$ from virtual heavy particles with mass, m , is

$$\begin{aligned} |A(q\bar{q} \rightarrow gh)|^2 &= 64g_s^2 \left(\frac{\hat{t}^2 + \hat{u}^2}{\hat{s}} \right) \left[C_1^2 + \frac{\hat{s}C_1C_5}{2} \right] \\ &= \lim_{m \rightarrow \infty} \left(\frac{4\alpha_s^3}{\pi} \right) \left(\frac{\hat{u}^2 + \hat{t}^2}{\hat{s}v^2} \right) | \mathcal{A}_5(\hat{s}, \hat{t}, \hat{u}, m^2) |^2, \end{aligned} \quad (20)$$

	Dirac Fermion	$SU(3)$ Triplet Scalar	$SU(3)$ Octet Scalar
$C_1(\Lambda)$	$\frac{\alpha_s \kappa_F}{12\pi v} \left[1 + \frac{7m_h^2}{120m_F^2} \right]$	$-\frac{\alpha_s}{96\pi M_S^2} C_h \left[1 + \frac{2m_h^2}{15M_S^2} \right]$	$-\frac{\alpha_s}{16\pi M_S^2} C_h \left[1 + \frac{2m_h^2}{15M_S^2} \right]$
$C_3(\Lambda)$	$-\frac{g_s \alpha_s \kappa_F}{360\pi v m_F^2}$	$-\frac{g_s \alpha_s}{1440M_S^4} C_h$	$-\frac{g_s \alpha_s}{240M_S^4} C_h$
$C_5(\Lambda)$	$\frac{11\kappa_F \alpha_s}{360\pi v m_F^2}$	$-\frac{\alpha_s}{360\pi M_S^4} C_h$	$-\frac{\alpha_s}{60\pi M_S^4} C_h$

TABLE I: The effective Lagrangian coefficient functions for heavy Dirac fermions and heavy scalars with mass, m_F and M_S , respectively. The coefficient functions, along with g_s and α_s , are evaluated at the scale $\Lambda = m_F, M_S$.

while the EFT amplitude for $gg \rightarrow gh$ from virtual heavy particles with mass, m , is

$$\begin{aligned}
|A(gg \rightarrow gh)|^2 &= g_s^2 \left[384C_1^2 \left[\frac{m_h^8 + \hat{s}^4 + \hat{t}^4 + \hat{u}^4}{\hat{s}\hat{t}\hat{u}} \right] + 1152C_1C_3m_h^4 \right] \\
&= \lim_{m \rightarrow \infty} \left(\frac{96\alpha_s^3}{\pi} \frac{m_h^8}{\hat{s}\hat{t}\hat{u}v^2} \right) \left\{ |\mathcal{A}_2(\hat{s}, \hat{t}, \hat{u}, m^2)|^2 + |\mathcal{A}_2(\hat{u}, \hat{s}, \hat{t}, m^2)|^2 \right. \\
&\quad \left. + |\mathcal{A}_2(\hat{t}, \hat{u}, \hat{s}, m^2)|^2 + |\mathcal{A}_4(\hat{s}, \hat{t}, \hat{u}, m^2)|^2 \right\}, \tag{21}
\end{aligned}$$

where \hat{s}, \hat{t} , and \hat{u} are the usual Mandelstam variables. The coefficient functions $\mathcal{A}_2(\hat{s}, \hat{t}, \hat{u}, m^2)$, $\mathcal{A}_4(\hat{s}, \hat{t}, \hat{u}, m^2)$ and $\mathcal{A}_5(\hat{s}, \hat{t}, \hat{u}, m^2)$ are given in Ref. [37] for fermion loops and in Ref. [41] for scalar loops. The C_1, C_3 and C_5 coefficients of Eqs. 20 and 21 depend in general on the parameters of the underlying UV completion of the model. By matching the EFT predictions with the heavy fermion expansions, we obtain the EFT coefficients given in Table I. At LO, the dimension -7 term contributing to the $gg \rightarrow gh$ amplitude does not contain any dependence on the kinematic variables. For TeV scale masses, it is clear that the coefficients are quite small. For the top partner model, the coefficient functions for the heavier Dirac fermion contributions need to be multiplied by the factor $\sin^2 \theta_L$ appearing in Eq. (19), while the SM top quark contribution is included exactly without using the EFT.

The matching of the EFT and the underlying UV theory are done at the high scale Λ . Using the anomalous dimensions found in Ref. [13, 54], the coefficients can be evolved to a low scale, $\mu_R \sim m_h$,

$$\frac{d}{d \ln \mu_R} \ln \left(\frac{C_1(\mu_R)}{g_s^2(\mu_R)} \right) = \mathcal{O}(\alpha_s^2(\mu_R)), \tag{22}$$

$$\frac{d}{d \ln \mu_R} \ln \left(\frac{C_3(\mu_R)}{g_s^3(\mu_R)} \right) = \frac{\alpha_s(\mu_R)}{\pi} 3C_A, \tag{23}$$

$$\frac{d}{d \ln \mu_R} \ln \left(\frac{C_5(\mu_R)}{g_s^2(\mu_R)} \right) = \frac{\alpha_s(\mu_R)}{\pi} \left(\frac{11}{6}C_A + \frac{4}{3}C_F \right), \tag{24}$$

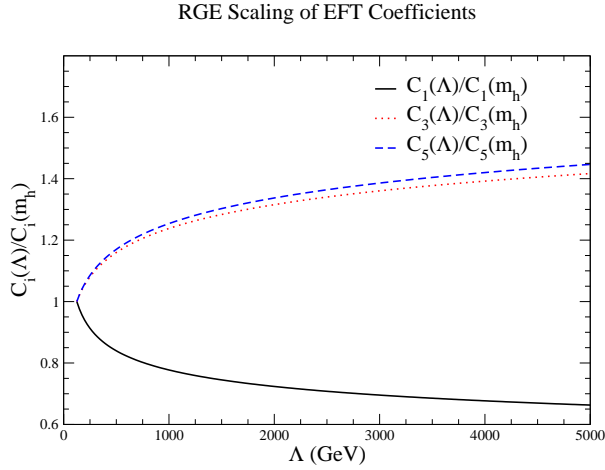


FIG. 2: The evolution of the dimension- 5 and dimension-7 EFT coefficients from the scale of new physics, $\sim \Lambda$, to the electroweak scale.

where $C_A = 3$ and $C_F = \frac{4}{3}$. The one-loop electroweak RG running of C_1/g_s^2 [55] is non-zero, and its effect on the Higgs p_T distribution in the TeV range is found to be at the percent level [56].

The leading-logarithmic solutions to the renormalization group running equations Eq. (22)-(24) are

$$C_1(\mu_R)/g_s^2(\mu_R) = C_1(\mu_0)/g_s^2(\mu_0), \quad (25)$$

$$C_3(\mu_R)/g_s^3(\mu_R) = \left(\frac{\alpha_s(\mu_R)}{\alpha_s(\mu_0)} \right)^{-\frac{3C_A}{2b_0}} \cdot C_3(\mu_0)/g_s^3(\mu_0), \quad (26)$$

$$C_5(\mu_R)/g_s^2(\mu_R) = \left(\frac{\alpha_s(\mu_R)}{\alpha_s(\mu_0)} \right)^{-\frac{1}{2b_0} \left(\frac{11}{6}C_A + \frac{4}{3}C_F \right)} \cdot C_5(\mu_0)/g_s^2(\mu_0), \quad (27)$$

where $b_0 = \frac{1}{12}(11C_A - 2n_{lf})$ and $\mu_0 \sim \Lambda$. The evolution of the coefficient functions is shown

in Fig. 2. C_1 is increased by \sim a factor of 2 when evolving from $\Lambda \sim 5$ TeV to the weak scale, while C_3 and C_5 are reduced by a similar factor.

IV. PHENOMENOLOGY

We will eventually be interested in whether measurements of the p_T spectrum can distinguish between the effects of the dimension-5 and dimension-7 operators resulting from scalars and from fermions; that is, *“Is the EFT a useful tool for disentangling the source of high scale physics?”*

Throughout this paper, diagrams involving the SM top quark are evaluated with exact m_t dependence without using the Higgs-gluon EFT, while the contributions from heavy BSM particles, such as a color triplet scalar or a fermionic top partner, are considered both exactly and in the EFT approximation.

A. Heavy Colored Scalars

We begin by considering the effect of heavy color triplet scalars on Higgs + jet production. (The case of a light colored scalar has been considered in [42].) We use CJ12 NLO PDFs [57] and $\mu_R = \mu_F = \sqrt{m_h^2 + p_T^2}$ for all curves, with $m_h = 125$ GeV, $m_t = 173$ GeV, and $m_b = 4.5$ GeV. All plots refer to Higgs + jet production at lowest order and with $\sqrt{s} = 14$ TeV. When using the EFT, the effects of heavy scalars are included using the coefficients of Table I. Since the effects are suppressed by $1/M_S^2$ in C_1 and $1/M_S^4$ in the other C_i , we expect relatively small effects unless the coefficient function C_h is large. We expect C_h to be of order the electroweak scale in a realistic model and in our plots, we take $C_h = 3M_Z$.¹ Numerically, the effects are linear in C_h for modest values of C_h/M_Z and our results can be trivially rescaled.

The exact one-loop contribution of the heavy scalars relative to the SM rate are shown in Fig. 3 and as expected, they cause only a few percent deviation from the SM rate at low p_T . We define the ratio, “BSM/SM” to be the differential (or integrated) rate in the theory

¹ If ϕ_i corresponds to the left-handed top squark of the MSSM, then in the alignment limit ($\sin \beta = \cos \alpha$), $C_h \sim 3M_Z$, which motivates our choice. This numerical value is not important for our conclusions, as long as C_h/M_Z is not a large number.

with the SM top quark and scalar included exactly normalized to the SM rate minus 1, i.e. it is the incremental contribution from the addition of a scalar. At large p_T , the deviation becomes significant, approaching $\sim 15\%$ for $p_T \sim 1$ TeV for a 500 GeV scalar and $\sim 5\%$ for a 1 TeV scalar. We note that the effects of a color octet scalar are a factor of $C_A/T_F = 6$ larger than those of a color triplet scalar. The integrated cross sections with a p_{Tcut} are shown in Fig. 4, and a significant contribution from the scalars to the boosted Higgs signal is apparent for $p_{Tcut} \sim M_S$ for $M_S = 500$ GeV. For the heavier scalar, $M_S \sim$ TeV, the effects are only a few % even for very large p_{Tcut} .

Since the lowest order contribution from scalars is known exactly, we can explore the range of validity of the EFT. Fig. 5 shows the deviation of the EFT calculation from the exact 1-loop result when color triplet scalars are included. For a 500 GeV scalar, the EFT is accurate to within a few % below M_S and has large deviations above 500 GeV when only the dimension-5 ($\sim 1/M_S^2$) contributions are included. Including the dimension-7 contributions improves the accuracy of the EFT. Interestingly, for $M_S = 1$ TeV, the EFT becomes less accurate at large p_T when the dimension-7 effects are included. The EFT expansion clearly breaks down at a scale $p_T \sim M_S$. Fig. 6 demonstrates the accuracy of the EFT in the p_T integrated cross section and we observe the same behavior. (The cross section is integrated to $p_T = 1$ TeV, where the EFT is breaking down. Since the partonic results are integrated with a falling PDF spectrum, we expect the results to be reasonably reliable.) The contributions from the gg and qg initial states are shown separately in Figs. 7 and 8.

B. Heavy Fermion Top Partners

In this section we consider the effect of a top partner model on the shape of the Higgs p_T distribution. We take the top partner mass $M_T = 500$ GeV and the mixing angle $\cos \theta_L = 0.966$. Fig. 9 shows the ratio of the inclusive cross section in the top partner model to that in the SM, minus 1, evaluated with the exact dependence on the masses m_t and M_T , along with the same quantity integrated with a P_{Tcut} . We note that the results of Ref. [22] demonstrate large effects at high $p_T \sim 1$ TeV when $\sin \theta_L = 0.4$. Regretably, such large mixing angles are excluded by precision electroweak data. (We agree with the results of Ref. [22] for small $\sin \theta_L$.) Fig. 10 shows the accuracy of the EFT predictions for differential and integrated p_T distributions, relative to the results with exact m_t and M_T dependence.

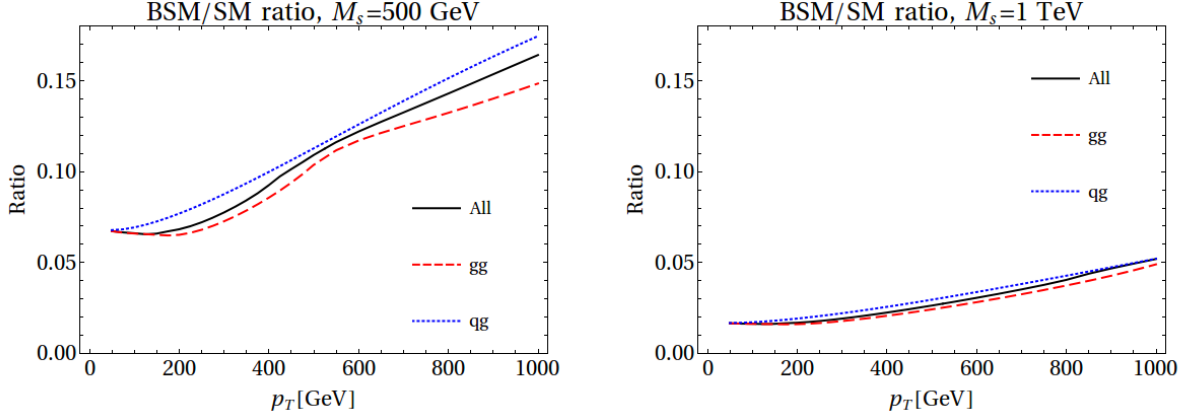


FIG. 3: Contribution of a 500 GeV color triplet scalar (LHS) and a 1 TeV scalar (RHS), relative to the SM Higgs p_T distribution. The gg and qg partonic channels, and the sum of all partonic channels (which also includes $q\bar{q}$), are shown separately. Both the SM top and the scalar contributions are included exactly at LO.

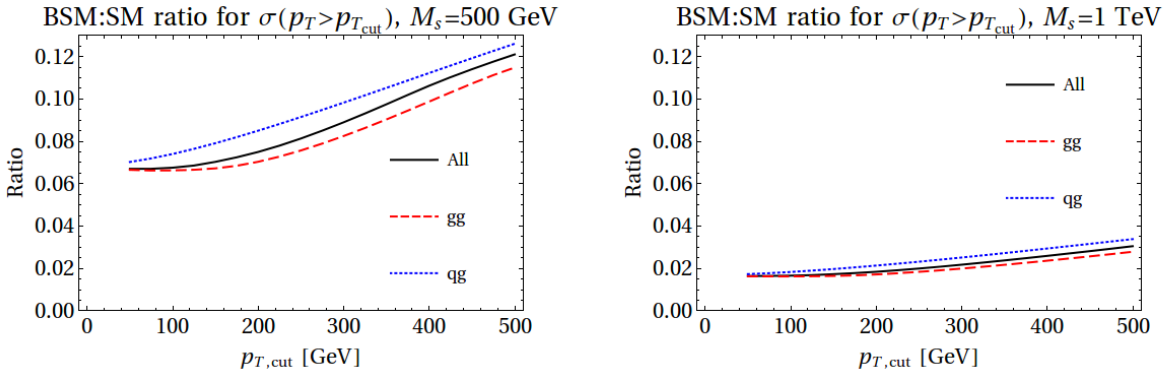


FIG. 4: Contribution of a 500 GeV color triplet scalar and a 1 TeV scalar, relative to the SM cross section, with a cut $p_{T,cut}$. The gg and qg partonic channels, and the sum of all partonic channels (which also include $q\bar{q}$), are shown separately. Both the SM top and the scalar contributions are included exactly at LO.

We close this section by summarizing our results for top partners and scalars in Fig. 11, which dramatically demonstrates the difficulty of extracting information about the underlying UV physics.

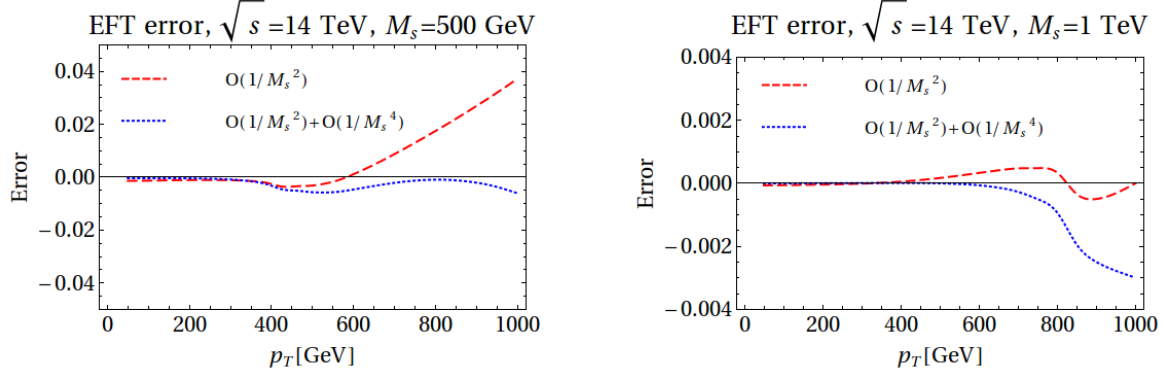


FIG. 5: Accuracy of the effective field theory calculation of $d\sigma/dp_T$ relative to the exact calculation when including 500 GeV (LHS) and 1 TeV (RHS) color triplet scalars including all partonic initial states. The dashed lines contain only the dimension-5 contributions, while the dotted lines contain both the dimension-5 and dimension-7 contributions. The SM top quark contribution is always included exactly.

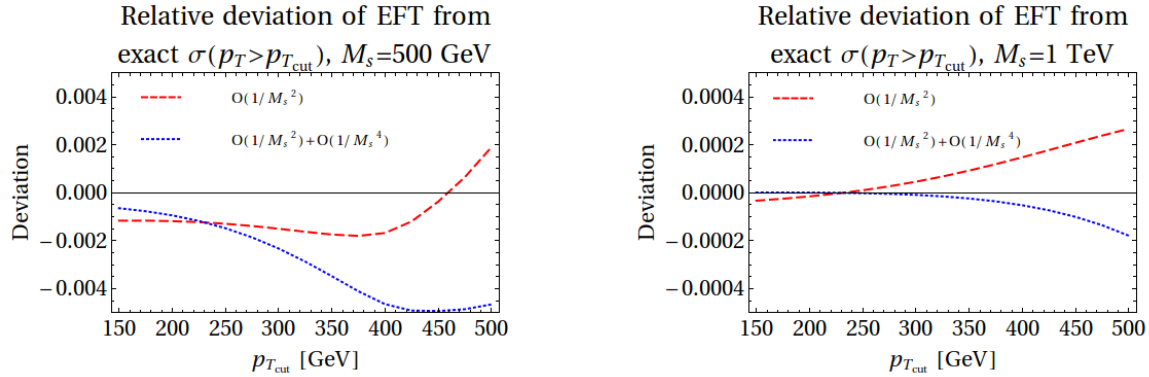


FIG. 6: Accuracy of the effective field theory calculation of the total cross section subject to a $p_{T,cut}$, relative to the exact calculation when including 500 GeV (LHS) and 1 TeV (RHS) color triplet scalars including all partonic initial states. The dashed lines contain only the dimension-5 contributions, while the dotted lines contain both the dimension-5 and dimension-7 contributions. The SM top quark contribution is included exactly.

C. EFT Fits

In this subsection, we consider the effects of a general rescaling of the EFT coefficients. As in Eq. (1) and Eq. (3), we consider the SM top quark contribution rescaled by κ_t , and the C_1 coefficients rescaled by κ_g relative to an infinitely heavy Dirac fermion whose mass

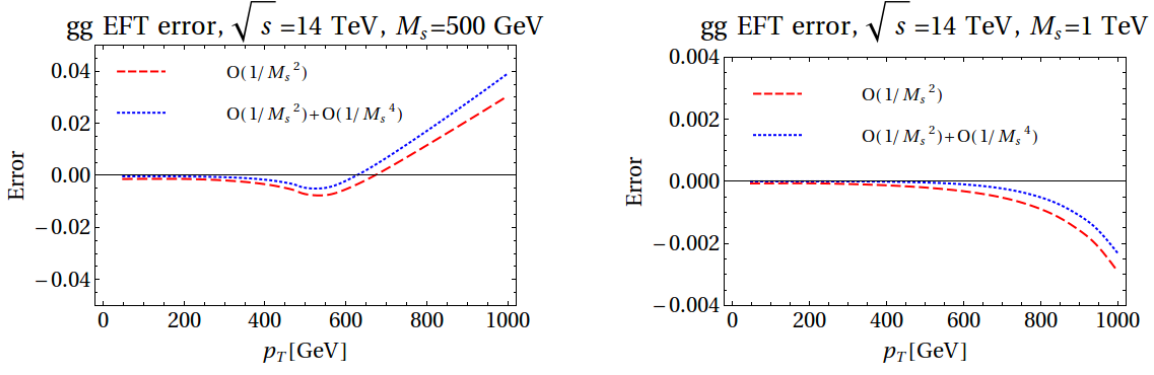


FIG. 7: Accuracy of the effective field theory calculation of $d\sigma/dp_T$ relative to the exact calculation when including 500 GeV (LHS) and 1 TeV (RHS) color triplet scalars and including only the gg initial state. The dashed lines contain only the dimension-5 contributions, while the dotted lines contain both the dimension-5 and dimension-7 contributions. The SM top quark contribution is included exactly.

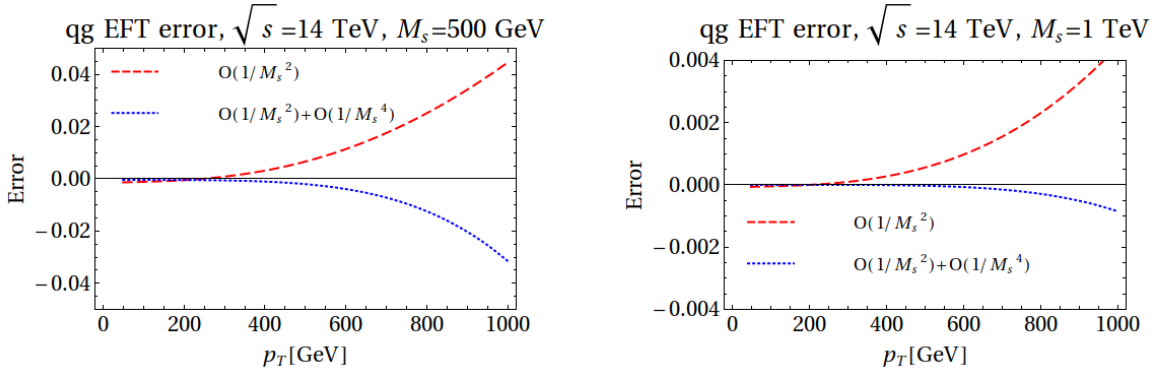


FIG. 8: Accuracy of the effective field theory calculation of $d\sigma/dp_T$ relative to the exact calculation when including 500 GeV (LHS) and 1 TeV (RHS) color triplet scalars and including only the qg initial state. The dashed lines contain only the dimension-5 contributions, while the dotted lines contain both the dimension-5 and dimension-7 contributions. The SM top quark contribution is included exactly.

comes entirely from the Higgs, i.e. $C_1 = \kappa_g \cdot \alpha_s / (12\pi v)$. For the dimension-7 operators, we vary the matching coefficients $C_i = \kappa_i C_i(M_S = 500 \text{ GeV}, C_h = 3m_Z)$ for $i = 3, 5$, where the reference values, scaled by κ_i , are $C_3(M_S, C_h) = -g_s \alpha_s C_h / (1440 M_S^4)$ and $C_5(M_S, C_h) = -\alpha_s C_h / (360\pi M_S^4)$ corresponding to the EFT coefficients from Table I for a 500 GeV scalar. The total cross section for single Higgs production is roughly unchanged from the SM, if we

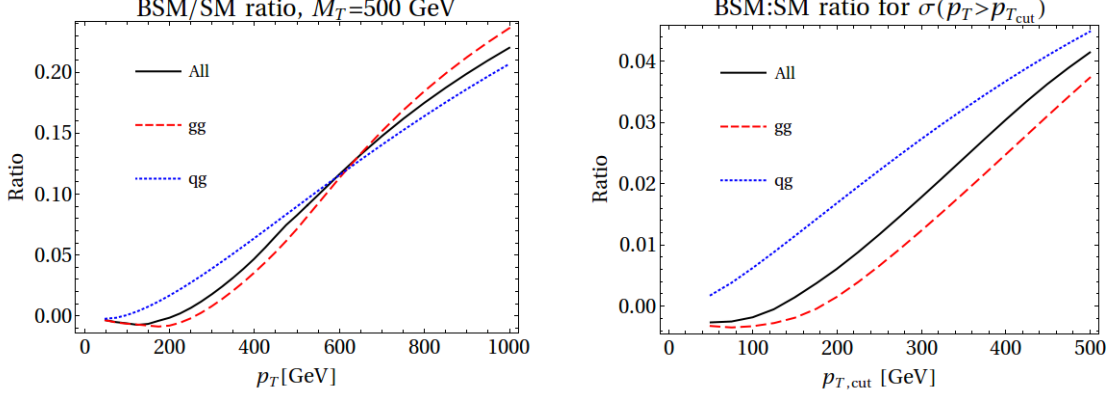


FIG. 9: The BSM contribution, relative to the SM contribution, to the differential (LHS) and integrated Higgs p_T distribution (RHS). The gg and qg partonic channels, and the sum of all partonic channels (which also include $q\bar{q}$), are shown separately. Both the top partner and top quark contributions are included exactly at LO.

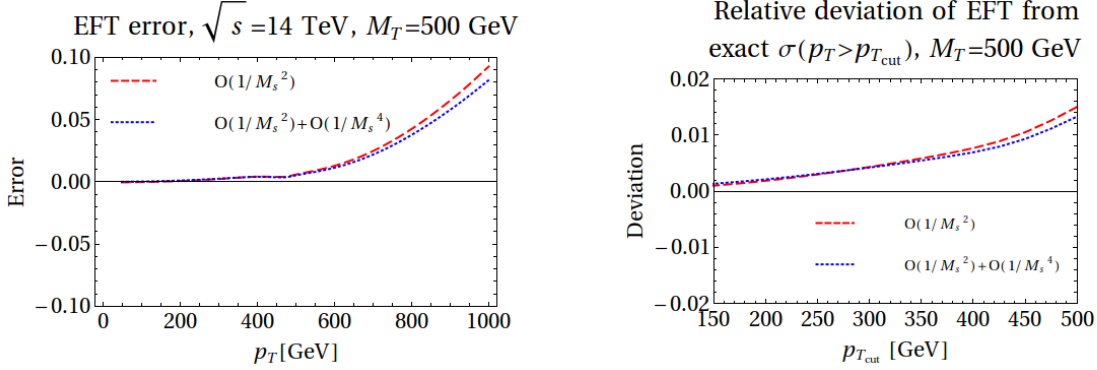


FIG. 10: Accuracy of the effective field theory calculation of the differential (LHS) and integrated (RHS) p_T distribution, relative to the exact calculation, for a 500 GeV fermionic top partner with $\theta = \pi/12$.

fix $\kappa_t + \kappa_g$ to be 1, according to Eq. (4). Fig. 12 demonstrates that excessively large values of κ_5 are required for a large effect from O_5 . Fig. 13 shows that the inclusion of O_3 has very little effect even for huge values of κ_3 , as expected from the helicity arguments in [13]. On the other hand, the effect of rescaling κ_t and κ_g separately can have a relatively large effect.

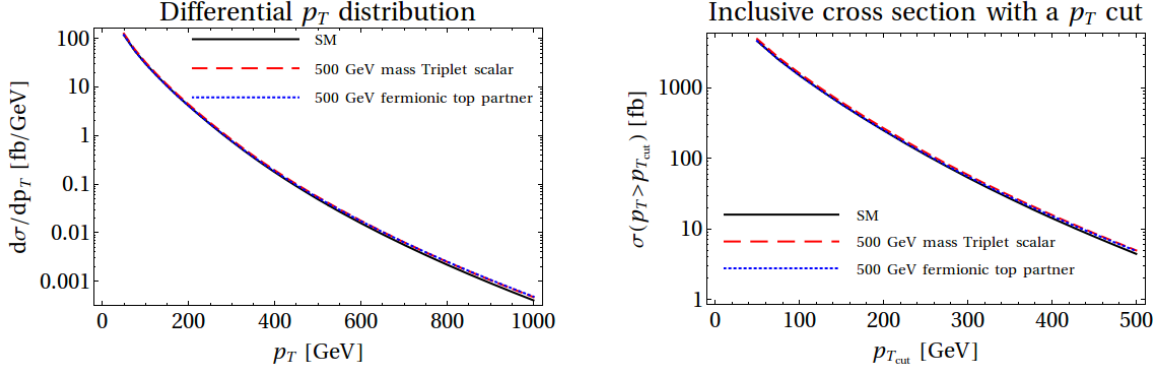


FIG. 11: Cross sections including the SM result and a 500 GeV color triplet scalar, the SM result and a 500 GeV top partner, compared with the SM predictions.

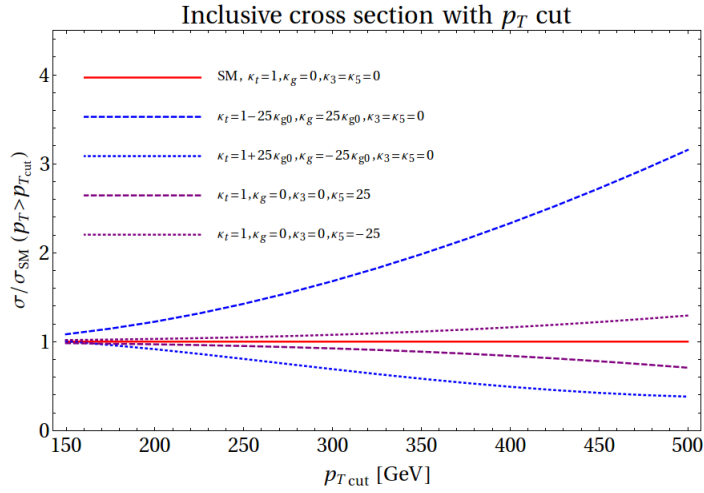


FIG. 12: Inclusive cross section with a p_T cut at $\sqrt{s} = 14$ TeV, normalized to the SM rate. In our parameterization of BSM effects, the SM rate is rescaled by κ_t , while C_1 , C_3 , and C_5 are rescaled by κ_g , κ_3 , and κ_5 , respectively, with the model in Subsection IV A corresponding to $|\kappa_g|/\kappa_{g0} = \kappa_3 = \kappa_5 = 1$, $\kappa_{g0} \approx 0.0337$. We have fixed $\kappa_t + \kappa_g = 1$ to approximately conserve the total cross section. κ_3 is fixed to zero in this plot to highlight the effects of κ_g and κ_5 .

V. CONCLUSION

The process Higgs + jet has been proposed as a useful channel for studying BSM physics and for disentangling the effects of a modification of the dimension-4 $t\bar{t}h$ Yukawa coupling

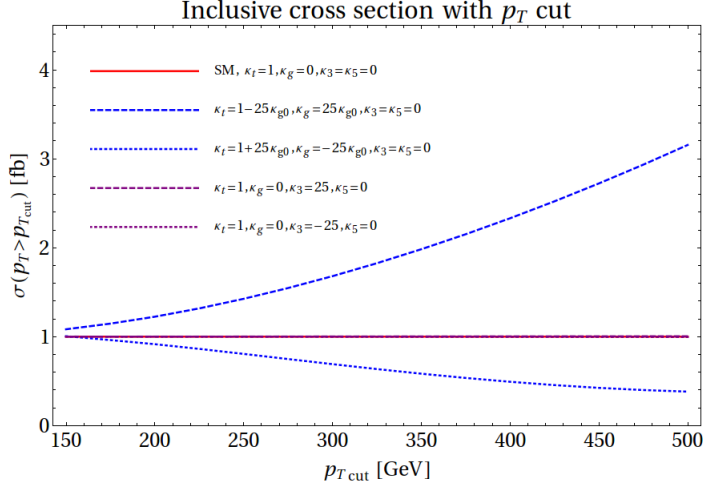


FIG. 13: Inclusive cross section with a p_T cut at $\sqrt{s} = 14$ TeV, normalized to the SM rate. In our parameterization of BSM effects, the SM rate is rescaled by κ_t , while C_1 , C_3 , and C_5 are rescaled by κ_g , κ_3 , and κ_5 , respectively, with the model in Subsection IV A corresponding to $|\kappa_g|/\kappa_{g0} = \kappa_3 = \kappa_5 = 1$, $\kappa_{g0} \approx 0.0337$. We have fixed $\kappa_t + \kappa_g = 1$ to approximately conserve the total cross section. κ_5 is fixed to zero in this plot to highlight the effects of κ_g and κ_3 . The effect of κ_3 can be seen to be extremely small.

from a non-SM dimension-5 Higgs-gluon effective vertex. We further include dimension-7 effective Higgs-gluon operators and compute the EFT coefficient functions in two representative models with heavy colored scalars and fermions. The coefficient functions are suppressed by inverse powers of the heavy mass scales, m , and are therefore quite small.

At lowest order, the effects of colored scalars and fermions can be computed exactly and the accuracy of the EFT determined. Typically, better accuracy is obtained in the gg channel than in the qg channel, and the EFT is accurate to a few percent for $p_T < m$. Our results illustrate the dilemma of the EFT approach: large effects are only obtained at high p_T and the contribution from the dimension -7 operators is small for $p_T < m$. On the other hand, Fig. 12 demonstrates a modest sensitivity to C_1 , independent of κ_t . If any deviation is found in the Higgs transverse momentum distribution up to 1 TeV, the deviation is unlikely to provide information about the UV physics beyond the single parameter C_1 . Our results support the validity of an approach using only the dimension-5 Higgs-gluon

operator. Inclusion of the NLO QCD corrections is unlikely to change this conclusion, since the NLO corrections to the C_1^2 contribution do not have a large p_T dependence in the region where the EFT is valid.

Acknowledgments

S.D. thanks A. Ismail and I. Low for discussions about the effects of virtual scalar particles. The work of SD and IL is supported the U.S. Department of Energy under grants No. DE-SC0012704 and DE-AC02-76SF00515. The work of MZ is supported by NSF grant PHY-1316617.

-
- [1] Tech. Rep. ATLAS-CONF-2014-009, CERN, Geneva (2014).
 - [2] Tech. Rep. CMS-PAS-HIG-14-009, CERN, Geneva (2014).
 - [3] S. Dittmaier et al. (LHC Higgs Cross Section Working Group) (2011), 1101.0593.
 - [4] S. Dittmaier, C. Mariotti, G. Passarino, R. Tanaka, et al. (2012), 1201.3084.
 - [5] K. Hagiwara, S. Ishihara, R. Szalapski, and D. Zeppenfeld, Phys.Rev. **D48**, 2182 (1993).
 - [6] S. Alam, S. Dawson, and R. Szalapski, Phys.Rev. **D57**, 1577 (1998), hep-ph/9706542.
 - [7] B. Henning, X. Lu, and H. Murayama (2014), 1412.1837.
 - [8] G. Giudice, C. Grojean, A. Pomarol, and R. Rattazzi, JHEP **0706**, 045 (2007), hep-ph/0703164.
 - [9] T. Corbett, O. Eboli, J. Gonzalez-Fraile, and M. Gonzalez-Garcia, Phys.Rev. **D86**, 075013 (2012), 1207.1344.
 - [10] A. Falkowski and F. Riva (2014), 1411.0669.
 - [11] J. Ellis, V. Sanz, and T. You, JHEP **1407**, 036 (2014), 1404.3667.
 - [12] C.-Y. Chen, S. Dawson, and C. Zhang, Phys.Rev. **D89**, 015016 (2014), 1311.3107.
 - [13] S. Dawson, I. Lewis, and M. Zeng (2014), 1409.6299.
 - [14] A. V. Manohar and M. B. Wise, Phys.Lett. **B636**, 107 (2006), hep-ph/0601212.
 - [15] T. Neumann and M. Wiesemann (2014), 1408.6836.
 - [16] B. A. Kniehl and M. Spira, Z.Phys. **C69**, 77 (1995), hep-ph/9505225.
 - [17] M. Spira, A. Djouadi, D. Graudenz, and P. Zerwas, Nucl.Phys. **B453**, 17 (1995), hep-ph/9504378.
 - [18] S. Dawson, Nucl.Phys. **B359**, 283 (1991).
 - [19] I. Low, R. Rattazzi, and A. Vichi, JHEP **1004**, 126 (2010), 0907.5413.
 - [20] C. Grojean, E. Salvioni, M. Schlaffer, and A. Weiler, JHEP **1405**, 022 (2014), 1312.3317.
 - [21] A. Azatov and A. Paul, JHEP **1401**, 014 (2014), 1309.5273.
 - [22] A. Banfi, A. Martin, and V. Sanz, JHEP **1408**, 053 (2014), 1308.4771.
 - [23] M. Buschmann, C. Englert, D. Goncalves, T. Plehn, and M. Spannowsky, Phys.Rev. **D90**, 013010 (2014), 1405.7651.
 - [24] M. Schlaffer, M. Spannowsky, M. Takeuchi, A. Weiler, and C. Wymant (2014), 1405.4295.
 - [25] M. Buschmann, D. Goncalves, S. Kuttimalai, M. Schonherr, F. Krauss, et al. (2014),

1410.5806.

- [26] R. V. Harlander and W. B. Kilgore, *Phys.Rev.Lett.* **88**, 201801 (2002), hep-ph/0201206.
- [27] C. Anastasiou and K. Melnikov, *Nucl.Phys.* **B646**, 220 (2002), hep-ph/0207004.
- [28] C. J. Glosser and C. R. Schmidt, *JHEP* **0212**, 016 (2002), hep-ph/0209248.
- [29] D. de Florian, M. Grazzini, and Z. Kunszt, *Phys.Rev.Lett.* **82**, 5209 (1999), hep-ph/9902483.
- [30] V. Ravindran, J. Smith, and W. L. van Neerven, *Nucl.Phys.* **B665**, 325 (2003), hep-ph/0302135.
- [31] V. Ravindran, J. Smith, and W. Van Neerven, *Nucl.Phys.* **B634**, 247 (2002), hep-ph/0201114.
- [32] R. Boughezal, F. Caola, K. Melnikov, F. Petriello, and M. Schulze, *JHEP* **1306**, 072 (2013), 1302.6216.
- [33] D. Neill (2009), 0908.1573.
- [34] R. V. Harlander and T. Neumann, *Phys.Rev.* **D88**, 074015 (2013), 1308.2225.
- [35] W. Buchmuller and D. Wyler, *Nucl.Phys.* **B268**, 621 (1986).
- [36] U. Baur and E. N. Glover, *Nucl.Phys.* **B339**, 38 (1990).
- [37] R. K. Ellis, I. Hinchliffe, M. Soldate, and J. van der Bij, *Nucl.Phys.* **B297**, 221 (1988).
- [38] D. Neill (2009), 0911.2707.
- [39] D. Ghosh and M. Wiebusch (2014), 1411.2029.
- [40] P. L. Cho and E. H. Simmons, *Phys.Rev.* **D51**, 2360 (1995), hep-ph/9408206.
- [41] R. Bonciani, G. Degrossi, and A. Vicini, *JHEP* **0711**, 095 (2007), 0709.4227.
- [42] C. Arnesen, I. Z. Rothstein, and J. Zupan, *Phys.Rev.Lett.* **103**, 151801 (2009), 0809.1429.
- [43] G. D. Kribs and A. Martin, *Phys.Rev.* **D86**, 095023 (2012), 1207.4496.
- [44] R. Boughezal and F. Petriello, *Phys.Rev.* **D81**, 114033 (2010), 1003.2046.
- [45] S. Gori and I. Low, *JHEP* **1309**, 151 (2013), 1307.0496.
- [46] L. Lavoura and J. P. Silva, *Phys.Rev.* **D47**, 1117 (1993).
- [47] J. Aguilar-Saavedra, *Phys.Rev.* **D67**, 035003 (2003), hep-ph/0210112.
- [48] J. Aguilar-Saavedra, R. Benbrik, S. Heinemeyer, and M. Prez-Victoria, *Phys.Rev.* **D88**, 094010 (2013), 1306.0572.
- [49] M. B. Popovic and E. H. Simmons, *Phys.Rev.* **D62**, 035002 (2000), hep-ph/0001302.
- [50] S. Dawson and E. Furlan, *Phys.Rev.* **D86**, 015021 (2012), 1205.4733.
- [51] S. Dawson, E. Furlan, and I. Lewis, *Phys.Rev.* **D87**, 014007 (2013), 1210.6663.
- [52] G. Aad et al. (ATLAS Collaboration), *JHEP* **1411**, 104 (2014), 1409.5500.

- [53] S. Chatrchyan et al. (CMS Collaboration), Phys.Lett. **B729**, 149 (2014), 1311.7667.
- [54] J. Gracey, Nucl.Phys. **B634**, 192 (2002), hep-ph/0204266.
- [55] C. Grojean, E. E. Jenkins, A. V. Manohar, and M. Trott, JHEP **1304**, 016 (2013), 1301.2588.
- [56] C. Englert and M. Spannowsky, Phys.Lett. **B740**, 8 (2014), 1408.5147.
- [57] J. Owens, A. Accardi, and W. Melnitchouk, Phys.Rev. **D87**, 094012 (2013), 1212.1702.